

RANDOM WALK APPROACH FOR SIMULATION OF PARTICLE DEPOSITION FROM TURBULENT FLOWS

Tamás KALMÁR NAGY* and David SWAILES**

*Department of Technical Mechanics
Technical University of Budapest
H-1521 Budapest, Hungary
email: kalmar@mm.bme.hu

**Department of Engineering Mathematics
University of Newcastle
Newcastle-upon-Tyne, UK
email: d.c.swailes@ncl.ac.uk

Received: May 14, 1996

Abstract

This study deals with a random walk simulation of particle transport and deposition from a stationary, isotropic turbulent flow: This is an implementation of the well-known Lagrangian approach, which treats the disperse phase as many particles. The trajectory of each particle is calculated according to the equations of the motion assuming a discrete eddy-field.

The ensemble-averaged quantities describe the behavior of the particle-fluid system, and these have been used to validate numerical solutions of a kinetic (probability density function transport) equation which models the same system. In this work we have only considered relatively large particles; particle-particle interactions and the influence of the particle phase on fluid phase have been neglected.

Keywords: particle deposition, random walk simulation.

1. Introduction

The task of predicting the deposition rate of solid particles or liquid droplets from a turbulent gas stream onto a surface is a common engineering problem in air cleaning, erosion of turbine blades, plate-out in nuclear reactor coolant circuits, etc.: other applications can be found in fields as diverse as occupational toxicology and river channel topology.

Mechanisms responsible for particle deposition include (but are not restricted to) inertial impaction, gravitational settling, electrostatic forces, lift forces, and diffusion. It has long been known that for electrostatically neutral particles with diameter in the range of a few μm the dominant mechanism is inertial impaction (KALLIO and REEKS, 1989).

There are two possible approaches for modelling particle deposition. The first is the Eulerian approach (also known as two-fluid approach), where the particles are treated as a continuous phase, hence one can derive the mass, energy, and momentum conservation equations. The second

choice is based on the Lagrangian approach, where trajectories of numerous individual particles are computed by solving the equations of motion, and the ensemble-averaged quantities describe the behavior of the particle–fluid system.

2. Steady-State Particle Transport in Turbulent Flows

A general kinetic equation for particle transport in turbulent fluid flow has recently been developed by REEKS (1991), and this study concerns the validation of a model for the steady-state deposition of high-inertia particles based on this equation.

Consider an axi-symmetric pipe in which the fluid flow is uniform and axial. For the sake of convenience we assume that the axis moves with the flow (i.e. with velocity \bar{u}).

Then the following form of the kinetic equation models the steady-state distribution of the particles normal to the boundary provided that the axial distribution of particles is uniform.

For large particles the kinetic equation reduces to a Fokker–Planck equation

$$\hat{v} \frac{\partial}{\partial \hat{y}} \hat{w}(\hat{y}, \hat{v}) + \frac{\partial}{\partial \hat{v}} [(\hat{v} - \hat{v}_g) \hat{w}(\hat{y}, \hat{v})] + \hat{\mu} \frac{\partial^2}{\partial \hat{v}^2} \hat{w}(\hat{y}, \hat{v}) = 0. \quad (1)$$

Here $\hat{w}(\hat{y}, \hat{v})$ is the ensemble-averaged phase-space particle density, \hat{y} is the perpendicular distance from the wall which bounds the flow, \hat{v} the wallward particle velocity, and \hat{v}_g the normal component of the gravitational settling velocity.

The variables and coefficients in this equation have been scaled using the characteristic particle response time τ^+ , and the local homogeneous particle velocity σ^+ , where σ^+ is determined by the diffusion coefficient μ^+ (at $\hat{y} = \hat{Y}$) as follows

$$\sigma^+ = \sqrt{\mu^+ \tau^+}.$$

The quantities denoted by $^+$ are given in wall units, i.e. they are non-dimensionalized by the friction velocity and the kinematic viscosity of the fluid (KALLIO and REEKS, 1989). In general σ^+ is spatially dependent, but for large particles it is approximately constant (equal to the value at the inlet) so that

$$\hat{v} = \frac{v^+}{\sigma^+}, \quad \hat{t} = \frac{t^+}{\tau^+}, \quad \hat{y} = \frac{y^+}{\sigma^+ \tau^+}, \quad \hat{Y} = \frac{Y^+}{\sigma^+ \tau^+}.$$

The variable y^+ is normalised with respect to $\sigma^+ \tau^+$, which represents a characteristic particle stop distance. Then \hat{Y} represents the number of

stop distances over which the transport is modelled (this is analogous to the interpretation in the kinetic theory of gas dynamics, where the domain size is considered in terms of the number of particle mean-free-paths).

To complete the model we must prescribe boundary conditions at $\hat{y} = 0$ and $\hat{y} = \hat{Y}$ (Fig. 1).

A boundary condition at $\hat{y} = \hat{Y}$ could be built on the assumption that at the inlet we have a constant source of particles with given positive velocity distribution.

Provided that \hat{Y} is sufficiently large, this asymptotic distribution will be approximately Gaussian with variance σ^{+2} . So it is natural to write the first boundary condition as

$$\hat{w}(\hat{Y}, \hat{v}) = n^* \sqrt{\frac{2}{\pi}} \exp\left(-\frac{\hat{v}^2}{2}\right) \quad \text{for} \quad \hat{v} > 0, \quad (2)$$

where n^* gives the concentration of particles with positive velocities at \hat{Y} (the inlet). For simplicity we set $n^* = 1$.

At the wall we have the flux balance

$$\hat{v}^- \hat{w}(0, \hat{v}^-) = - \int \hat{v}^+ \hat{w}(0, \hat{v}^+) \Theta(\hat{v}^+ | \hat{v}^-) d\hat{v}^+ \quad \text{for} \quad \hat{v}^- < 0, \quad (3)$$

where $\Theta(\hat{v}^+ | \hat{v}^-)$ denotes the conditional probability density relating the transition of a positive particle velocity from \hat{v}^+ to a negative one (\hat{v}^-) after collision.

So this boundary condition depends on the form of Θ . We have considered a simple deterministic process, which includes some energy loss during particle-wall collisions. Furthermore, if the impact velocity of a particle is smaller than a given critical velocity then that particle is adsorbed. The rebound velocity is given by

$$\hat{v}^- = -\sqrt{\hat{v}^{+2} - \hat{v}_c^2} \quad \hat{v}^+ > \hat{v}_c,$$

where \hat{v}_c is the critical impact velocity. This gives

$$\hat{w}(0, \hat{v}^-) = w(0, \hat{v}^+), \quad \hat{v}^+ > \hat{v}_c. \quad (4)$$

Note that the value of \hat{v}_c determines the type of the boundary, i.e. in the case $\hat{v}_c = 0$ the surface is perfectly reflecting (no energy loss, no adsorption), while $\hat{v}_c \rightarrow \infty$ corresponds to a perfectly adsorbing boundary.

A brief description of the numerical method for solving this two-point boundary value problem is given in Appendix A.

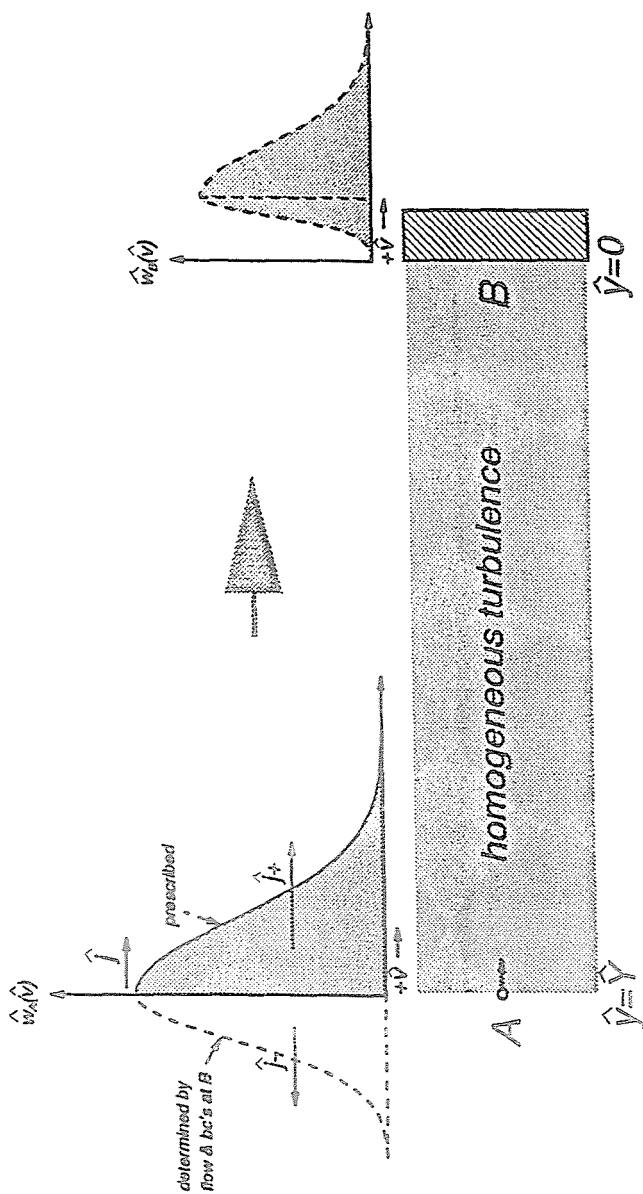


Fig. 1. Deposition in homogeneous turbulence: Phase-space distributions at projection point A and at wall B for perfect adsorption

3. Important Quantities

In studying solutions to the model given by Eqs. (1), (2) and (4) the following quantities are of interest.

The current:

$$\hat{j}(\hat{y}) = \int_{-\infty}^{\infty} \hat{v}\hat{w}(\hat{y}, \hat{v})d\hat{v}.$$

The concentration:

$$\hat{\rho}(\hat{y}) = \int_{-\infty}^{\infty} \hat{w}(\hat{y}, \hat{v})d\hat{v}.$$

The average particle concentration:

$$\langle \hat{\rho} \rangle = \frac{1}{\hat{Y}} \int_0^{\hat{Y}} \hat{\rho}(\hat{y})d\hat{y}.$$

The deposition rate:

$$\hat{k} = \frac{\hat{j}(0)}{\langle \hat{\rho} \rangle} = \frac{\int_{-\infty}^{\infty} \hat{v}\hat{w}(0, \hat{v})d\hat{v}}{\frac{1}{\hat{Y}} \int_0^{\hat{Y}} \int_{-\infty}^{\infty} \hat{w}(\hat{y}, \hat{v})d\hat{v}d\hat{y}}.$$

Further it is of great theoretical and practical interest to consider the particle velocity distribution at the wall. This is given by

$$\hat{\Phi}(\hat{v}) = \frac{\hat{w}(0, \hat{v})}{\int_{-\infty}^{\infty} \hat{w}(0, \hat{v})d\hat{v}}.$$

In this study a comparison is made between the values of these quantities as predicted by numerical solution of the kinetic model and the following approximations derived from the random walk simulation (outlined in the next section).

The current:

$$j(y_i) \cong \frac{1}{M\delta y} \sum_j v_j \bar{n}_{ij}$$

where \bar{n}_{ij} is the time-averaged number of particles in bin centered on (y_i, v_j) and

$$M = \sum_i \sum_j \bar{n}_{ij}.$$

The concentration $\rho(y)$ is approximated from the simulation as

$$\rho(y_i) \cong \frac{c}{\sqrt{2\pi}} \frac{1}{\delta y} \sum_j \bar{n}_{ij},$$

where c is the delay time between particle release and can be thought as a transformation in the time variable (thus compensates for delay-time effects).

The $\frac{1}{\sqrt{2\pi}}$ term is needed to normalise the inlet velocity distribution relative to the boundary condition (2).

The average concentration:

$$\langle \rho \rangle \cong \frac{1}{Y} \sum_i \rho(y_i) \delta y.$$

The deposition rate:

$$k = \frac{j(0)}{\langle \rho \rangle}.$$

The velocity distribution: If the number of particles in bin v_j at the wall is denoted by \bar{n}_j in the simulation then

$$w(0, v_j) \cong \frac{1}{\delta v} \bar{n}_j,$$

where δv is the width of the bin in the v direction, so the velocity distribution function has the form

$$\Phi(v_j) \cong \frac{1}{\delta v} \frac{\bar{n}_j}{\sum_j \bar{n}_j}.$$

4. Random Walk Simulation

We simulate the turbulent flow as a discrete eddy-field. Each eddy has some carrier velocity u and a specified life-time ΔT .

Since high-inertia particles will not be significantly influenced by turbulence in the near-wall region, we may approximate the eddy lifetime and the carrier velocity as seen by the particles as spatially independent (boundary layer effects only play role for small particles).

For the simulation it is easiest to work in terms of these fluid characteristics, i.e. to scale the velocities on σ_u^\dagger (the rms velocity of the fluid),

times on τ_L^+ (the Lagrangian integral time-scale), and the spatial variable on $\sigma_u^+ \tau_L^+$ (the stop distance), as follows

$$v = \frac{v^+}{\sigma_u^+}, \quad t = \frac{t^+}{\tau_L^+}, \quad y = \frac{y^+}{\sigma_u^+ \tau_L^+}, \quad Y = \frac{Y^+}{\sigma_u^+ \tau_L^+}, \quad u = \frac{u^+}{\sigma_u^+}, \quad v_g = \frac{v_g^+}{\sigma_u^+}$$

The equations for particle motion are then given by

$$\dot{y}(t) = v(t),$$

$$\dot{v}(t) = \gamma [(u - v(t)) + v_g], \tag{5}$$

where y is the position, v is the particle velocity, u is the carrier flow velocity v_g is the gravitational settling velocity.

γ^{-1} is the particle response time given by

$$\gamma = \frac{\tau_L^+}{\tau^+},$$

where τ^+ is the particle relaxation time (in wall units). For large particles we have $\tau^+ \gg 100$ and, from KALLIO and REEKS (1989) we see that $\tau_L^+ \leq 100$ so that $\gamma \ll 1$. In this work we have set $\gamma = 0.01$ throughout.

The $\gamma(u - v(t))$ term corresponds to a Stoke's drag assumption from which it is clear that the velocity of a particle will not change much crossing an eddy neglecting the gravitational effect (vertical pipe).

We model the autocorrelation of u as exponentially decaying and, in view of the normalisation, with a unit integral time-scale, so we can choose the fluid velocity from a standard normal distribution and the eddy-lifetime from the exponential distribution (with unit mean).

To get the equilibrium particle distribution given by the boundary condition (2) the initial velocities must be drawn from the distribution $v \exp\left(-\frac{v^2}{2}\right)$. The time averaged particle distribution at the inlet will then conform the required half-Gaussian (consider a finite width strip at the inlet, the particle residence time then is inversely proportional to its velocity).

So we should take

$$v_{inlet} = \sqrt{-2 \ln(z)},$$

$$\Delta T = -\ln(q),$$

where z , q are uniformly distributed random numbers from (0,1).

The initial velocities must be scaled to achieve the correct particle rms velocity relative to the fluid rms velocity (see section 5).

Integrating system (5) yields:

$$\begin{aligned} y(t) &= y_0 + \left(u + \frac{v_g}{\gamma}\right)t + \frac{1}{\gamma} \left[v_0 - \left(u + \frac{v_g}{\gamma}\right) \right] (1 - e^{-\gamma t}), \\ v(t) &= \left(u + \frac{v_g}{\gamma}\right) + \left[v_0 - \left(u + \frac{v_g}{\gamma}\right) \right] e^{-\gamma t}, \end{aligned} \quad (6)$$

where v_0 denote the initial particle position and velocity, respectively.

We can imagine the trajectory of the motion as a curve in the three-dimensional (y, v, t) phase-space.

By discretising this phase-space (i.e. discretising the state variables) we can extract information about the average particle behavior based on the quantities specified in section 3. This can be achieved by storing this discretized phase-space (the 'cube').

(We note that storing the whole cube is only necessary when we are interested in phase-space density distributions, otherwise we can define two- and one-dimensional arrays for storing 'projected' information).

Because of memory limitations the cube should be defined for $0 \leq y \leq Y$, $v_{\min} \leq v \leq v_{\max}$ and $0 \leq t \leq t_{\max}$.

Hence our discretised phase-space consists of small cells (bins) with sides δ_y , δ_v , δ_t in the y, v , and t directions, respectively.

So we solve system (5) for a given initial velocity, carrier velocity and eddy-lifetime with time step δ_t . After each timestep we increase the content of the corresponding bin by 1.

When the eddy-lifetime expires we simulate another and a new carrier velocity.

We follow the trajectory till the particle is either adsorbed at the wall or leaves the cube.

We maintain a constant particle release rate (this means that the n th particle starts at time $t_{start} = n \cdot c$, where c is the delay time between particle releases) into the flow during the process. Varying the release rate allows an equilibrium state to be achieved within a feasible time-scale.

Without going into details, we present solutions to some of the problems that were identified during this work.

We must determine the time (impact time) when the particle hits the wall and since Eq. (6) is nonlinear we have used a bisection method to establish this instant.

Also because of the nonlinearity, we should be careful, since the particle can leave and re-enter the phase-space during one time step.

To avoid this we determine the position of the particle when the sign of its velocity changes, i.e. the value of t such that

$$v(t) = 0 = u + \frac{v_g}{\gamma} + \left[v_0 - \left(u + \frac{v_g}{\gamma} \right) \right] e^{-\gamma t}. \quad (7)$$

It can be shown that $y(t)$ does have an extremum if

$$v_0 \left(u + \frac{v_g}{\gamma} \right) < 0.$$

Solving (7) for t we get

$$t = -\frac{1}{\gamma} \ln \left[\frac{u + \frac{v_g}{\gamma}}{u + \frac{v_g}{\gamma} - v_0} \right].$$

With this and (6) we can check the position of the particle (provided that this time is smaller than the eddy-lifetime).

By adjusting the particle release rate c and the time-step δt , equilibrium states were generated in the simulation process. This was ascertained by consideration of the mass M as a function of time, see *Fig. 2*.

When M is roughly constant, we average the quantities over an appropriate time interval, hence we obtain the steady-state solution.

It is clear from the nature of Monte-Carlo simulations that the more particles one uses, the less the noise. So the implementation allowed for the possibility of releasing more particles into the flow at the same time. *Fig. 3* shows a comparison of results from two simulations using 1 and 10 particle releases.

5. Comparison of the Simulation Results with Numerical Solutions

To compare the solutions from the random walk simulation and the kinetic equation we need to relate the two scalings. This connection is given by (see SWAILES and REEKS, 1994b)

$$\sigma^+ = \frac{\sigma_u^+}{\sqrt{1 + \frac{\tau^+}{\tau_L^+}}}.$$

In the simulation we solve the equations of motion scaled on fluid characteristics

$$\dot{v}(t) = \gamma [(v(t) - u) + v_g],$$

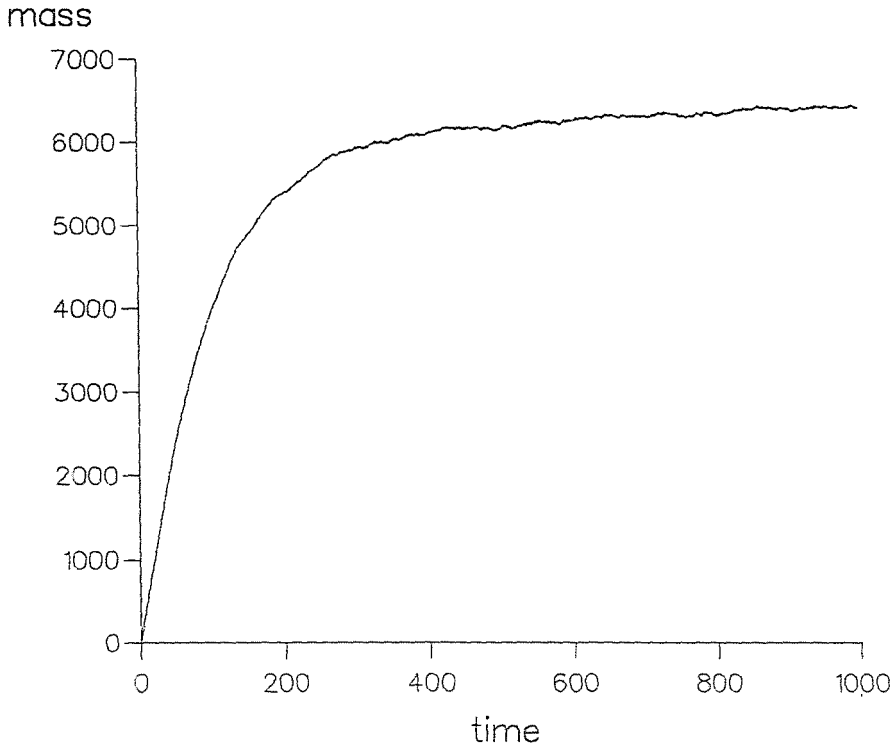


Fig. 2. The number of particles (mass) as a function of time

where

$$\gamma = \frac{\tau_L^+}{\tau^+}.$$

Hence

$$\sigma^+ = \frac{\sigma_u^+}{\sqrt{1 + \gamma^{-1}}}.$$

This gives

$$\hat{v} = v \sqrt{\frac{1 + \gamma}{\gamma}} \quad \text{and} \quad \hat{y} = y \sqrt{\gamma(1 + \gamma)}$$

which define the relationship between the two coordinate systems.

Since k^+ has units of velocity it follows that

$$\hat{k} = \frac{k^+}{\sigma^+}$$

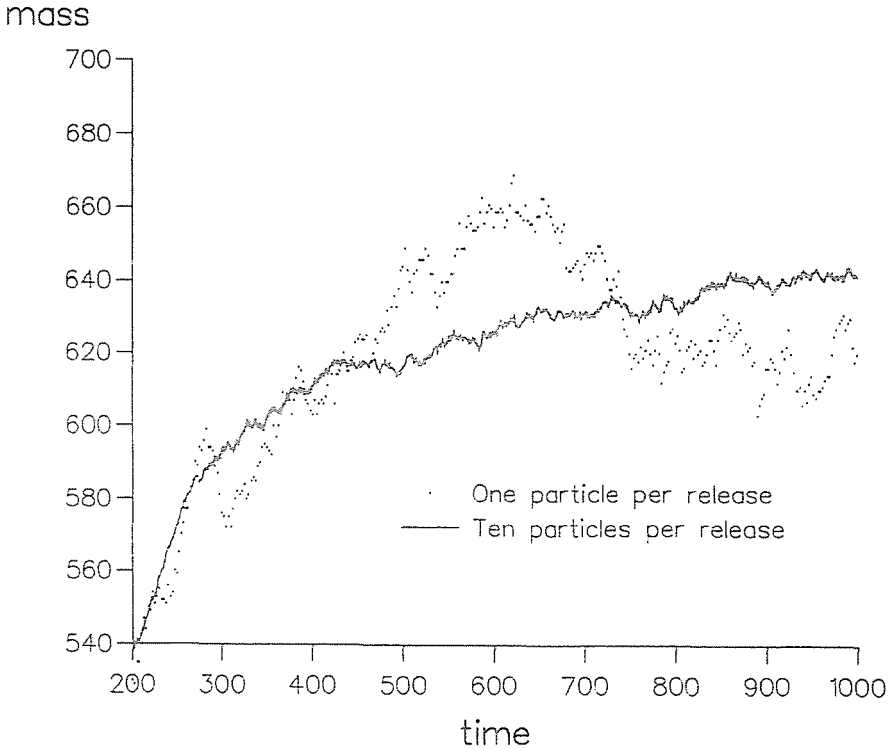


Fig. 3. The effect of noise reduction

We can demonstrate this formally from the definition

$$k^+ = \frac{j^+}{\rho^+}$$

as follows

$$k^+ = \frac{j^+}{\rho^+} = \frac{\int \nu^+ w^+ d\nu^+}{\frac{1}{\bar{Y}^+} \sigma^{+2} \int w^+ d\nu^+ dy^+} = \frac{\int \hat{\nu} \sigma^+ w \sigma^+ d\hat{\nu}}{\frac{1}{\sigma^+ \tau^+ \bar{Y}^+} \int w \sigma^+ d\nu \sigma^+ \tau^+ d\hat{y}} =$$

$$\frac{\int \hat{\nu} w d\hat{\nu}}{\frac{\sigma^+}{\bar{Y}^+} \int w d\nu d\hat{y}} = \sigma^+ \hat{k}.$$

Consequently we get

$$k = \frac{k^+}{\sigma_u^+} = \frac{\hat{k} \sigma^+}{\sigma_u^+} = \hat{k} \frac{1}{\sqrt{1 + \gamma^{-1}}}.$$

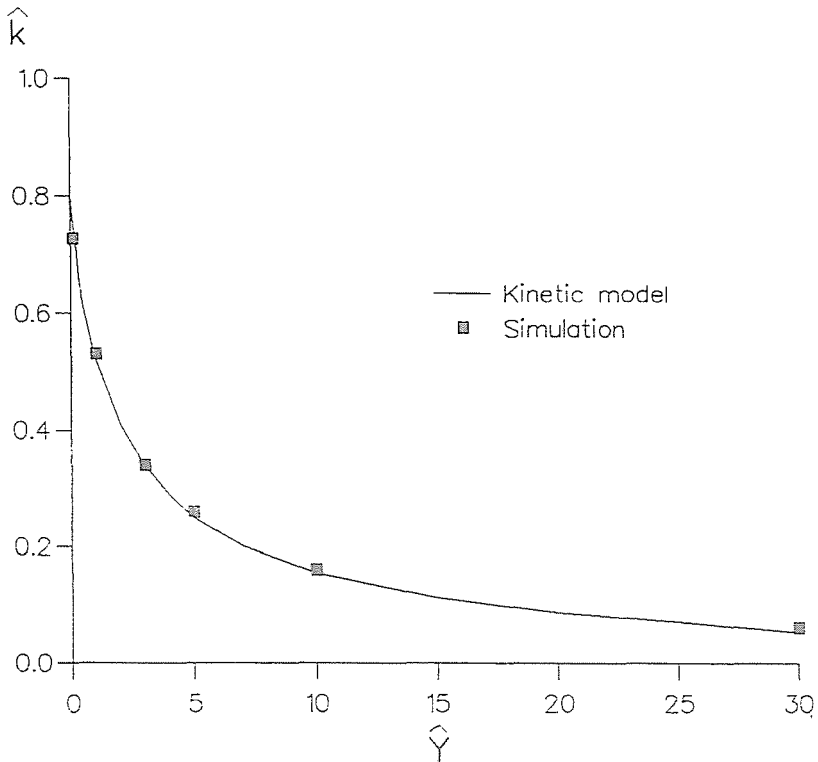


Fig. 4. Dependence of the deposition rate on mean-free path

Fig. 4 shows the value of deposition rate for a range of \hat{Y} values with a perfectly adsorbing boundary.

The program for solving the kinetic equation was only able to calculate \hat{k} for $\hat{Y} \geq 0.3$ so for $\hat{Y} = 0$ we took $\hat{k} = \sqrt{\frac{2}{\pi}}$ (SWAILES and REEKS, 1994a).

Similarly for the concentration

$$\hat{\rho} = \frac{\sigma_u^+}{\sigma^+} \rho = \sqrt{1 + \gamma^{-1}} \rho$$

Fig. 5 shows the spatial concentration for various \hat{Y} values.

Note that the concentration approaches $\frac{1}{2}$ across the pipe as \hat{Y} decreases.

As \hat{Y} increases the distribution at the injection point approximates the standard normal distribution. Consequently the particle concentration at this point increases from $\frac{1}{2}$ to unity. In addition, as \hat{Y} increases, the concentration profile will decrease linearly over a greater proportion of the domain, so that the concentration at the wall necessarily reduces to zero.

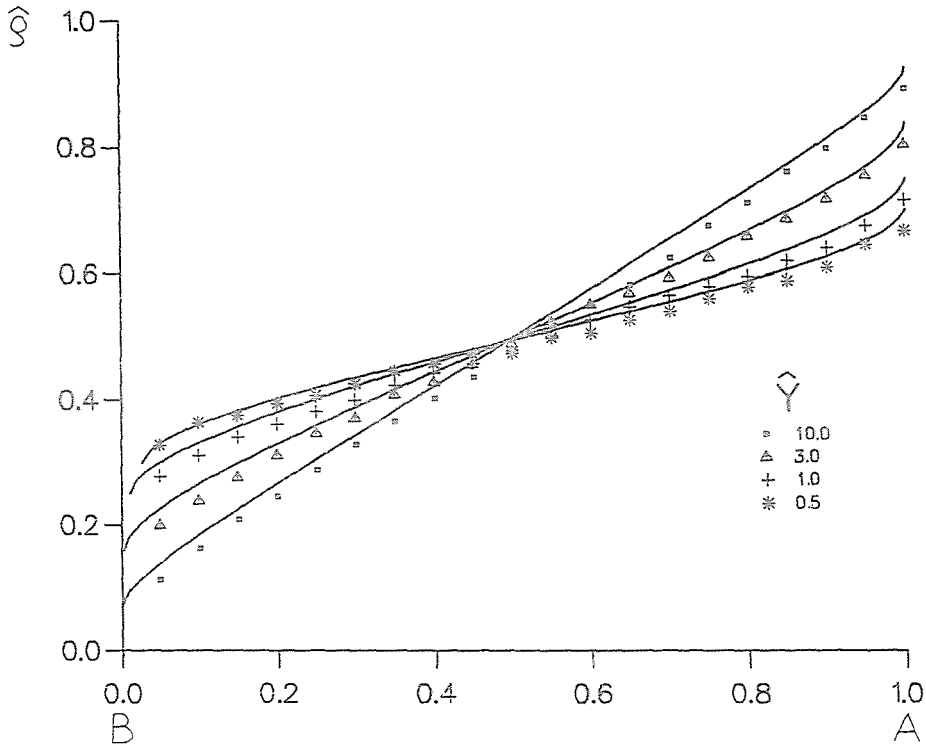


Fig. 5. Dependence of spatial particle concentration on \hat{Y}

Note also the interesting result that $\hat{\rho} \left(\frac{\hat{Y}}{2} \right) = \frac{1}{2}$ for all values of \hat{Y} . This is due to the ‘persistence’ of the Gaussian distribution across the domain – this is evident in Fig. 5, and is also reflected in Fig. 6 which shows values of the mean velocity (inversely related to $\hat{\rho}$), and the particle rms velocity as functions of distance from the wall, and for a range of values of \hat{Y} . The figure also shows values obtained by simulation.

The relationship between particle velocity distributions at the wall is given by

$$\hat{\Phi}(\hat{v}) = \sqrt{\frac{\gamma}{1 + \gamma}} \Phi(v).$$

Effects of interactions between the critical impact velocity v_c and the gravitational settling velocity v_g are shown in Figs. 7 and 8. Fig. 7 shows the particle velocity distribution at the wall for $v_c = 3$ and $v_g = 5$, while Fig. 8 depicts the distribution for $v_c = 5$ and $v_g = 5$. In both cases $\gamma = 10$.

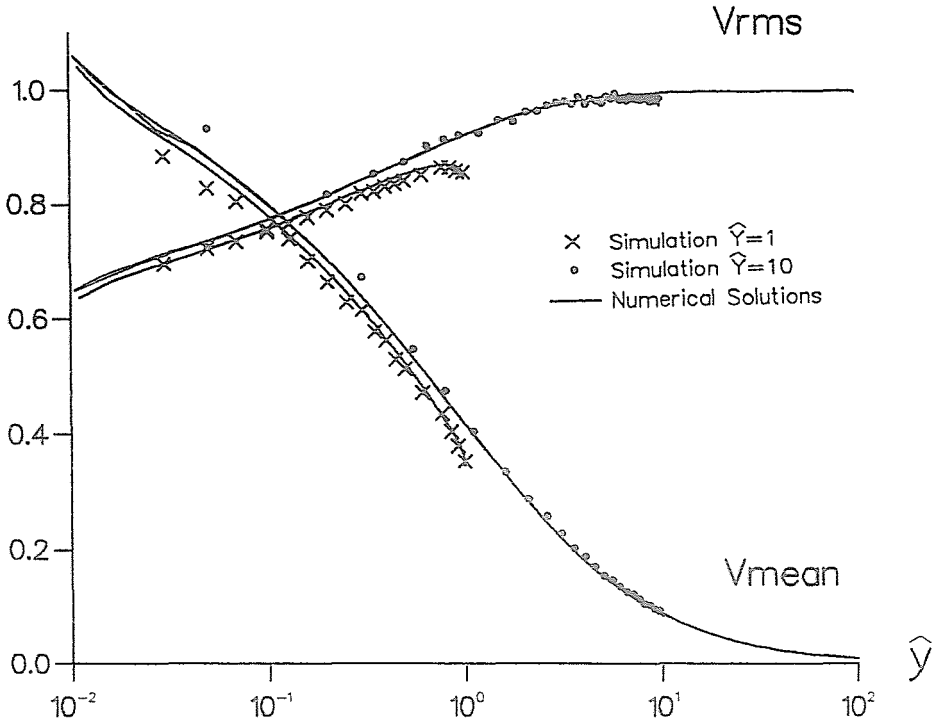


Fig. 6. Spatial variation in mean and rms particle velocities

Fig. 9 and 10 show phase-space distributions for $v_c = 5$ and $v_c = 3$, respectively ($v_g = 5$ and $\hat{Y} = 1$ were used in both cases), while a typical phase-space distribution for a perfectly adsorbing boundary is shown in Fig. 11. The two pictures in the figures correspond to simulation and numerical solution (from left to right). Note the difference at the wall, which is due to the finite width of cells in the simulation.

6. Conclusion

The simulations performed gave excellent agreement with numerical solutions of the steady-state kinetic equation obtained by a spectral method. In this respect the simulation results can be regarded as validating the kinetic equation.

The advantage of the random walk approach is that other deposition mechanism and forms of boundary conditions can easily be built into the

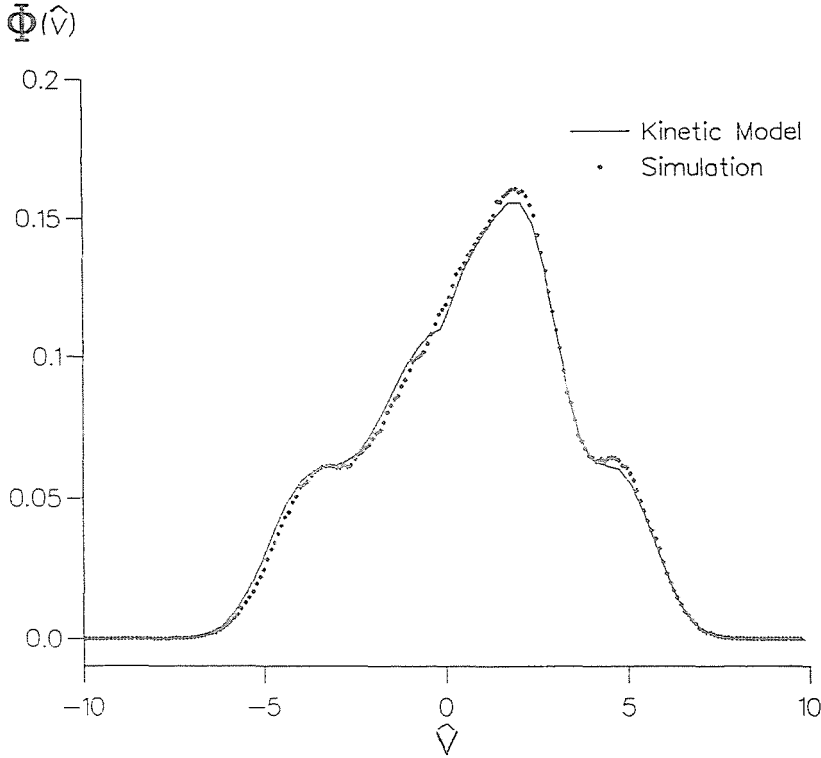


Fig. 7. Velocity distribution at partially adsorbing boundary

simulation. However, more CPU time is required than is needed for solving the corresponding boundary-value problem given by the kinetic equation.

Appendix A Spectral Method for Solving the Kinetic Equation

Approximate solutions for the kinetic equation can be found (for further details see SWAILES and REEKS, REEKS et al., 1991) in the form

$$\hat{w}(\hat{y}, \hat{v}) \approx \sum_{n=0}^N \phi_n(\hat{y}) \psi_n(\hat{v}) \quad (\text{A1})$$

where ψ_n s are orthonormal Hermite functions.

Making this approximation exact at collocation points v_0, \dots, v_N - the zeros of ψ_{N+1} - leads to a first order system $PW' = QW$ with $W = (w_0(\hat{y}, v_0), \dots, w_N(\hat{y}, v_N))$.

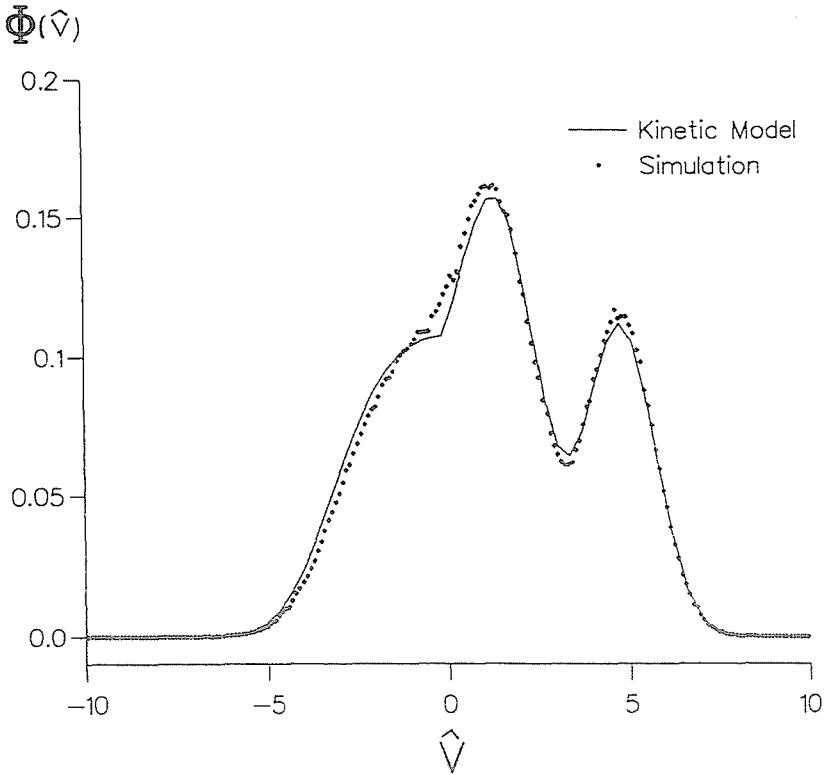


Fig. 8. Velocity distribution at partially adsorbing boundary

The matrices \mathbf{P} and \mathbf{Q} involve the diffusion coefficient $\hat{\mu}$, so in general they are spatially dependent (however, during this study we have considered large particles, for which the approximation $\hat{\mu} = 1$ is valid (REEKS, 1991)). This reduces \mathbf{P} to a diagonal form $diag(v_n)$, hence the first order system for W can be written as $W' = P^{-1}QW$.

The boundary conditions for this system at $\hat{y} = \hat{Y}$ follow from (2), and at $\hat{y} = 0$ from (4) using the fact that the transformation $\Phi \mapsto W$ determined by (A1) is invertible. This boundary-value problem then can be solved numerically. (The numerical solutions with which we compared the results of the random walk simulation were obtained by using an adaptive finite-difference scheme with deferred correction provided by NAG routine D02GBF (GLADWELL, 1987)).

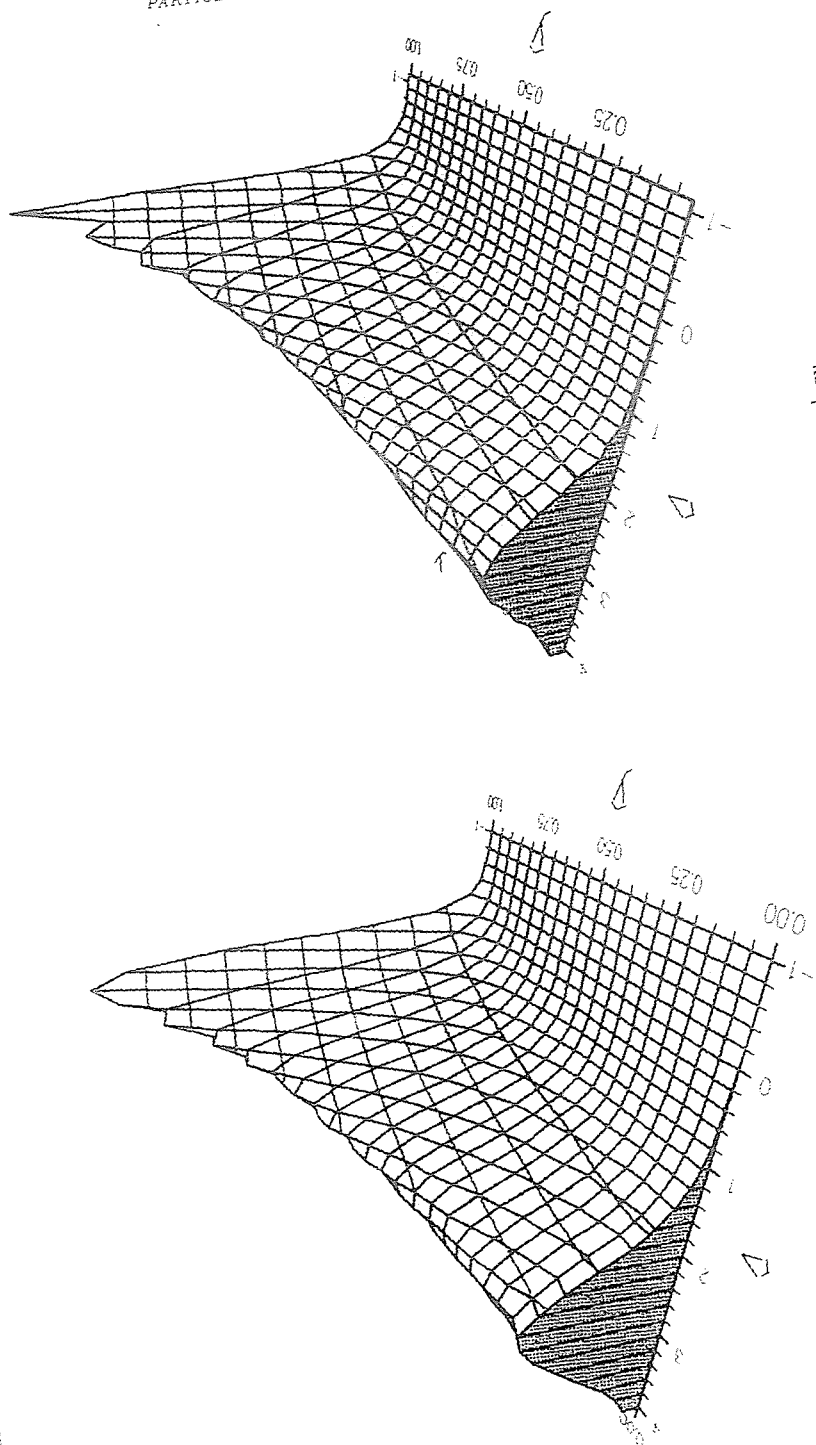


Fig. 9. Phase-space distribution for partially adsorbing boundary

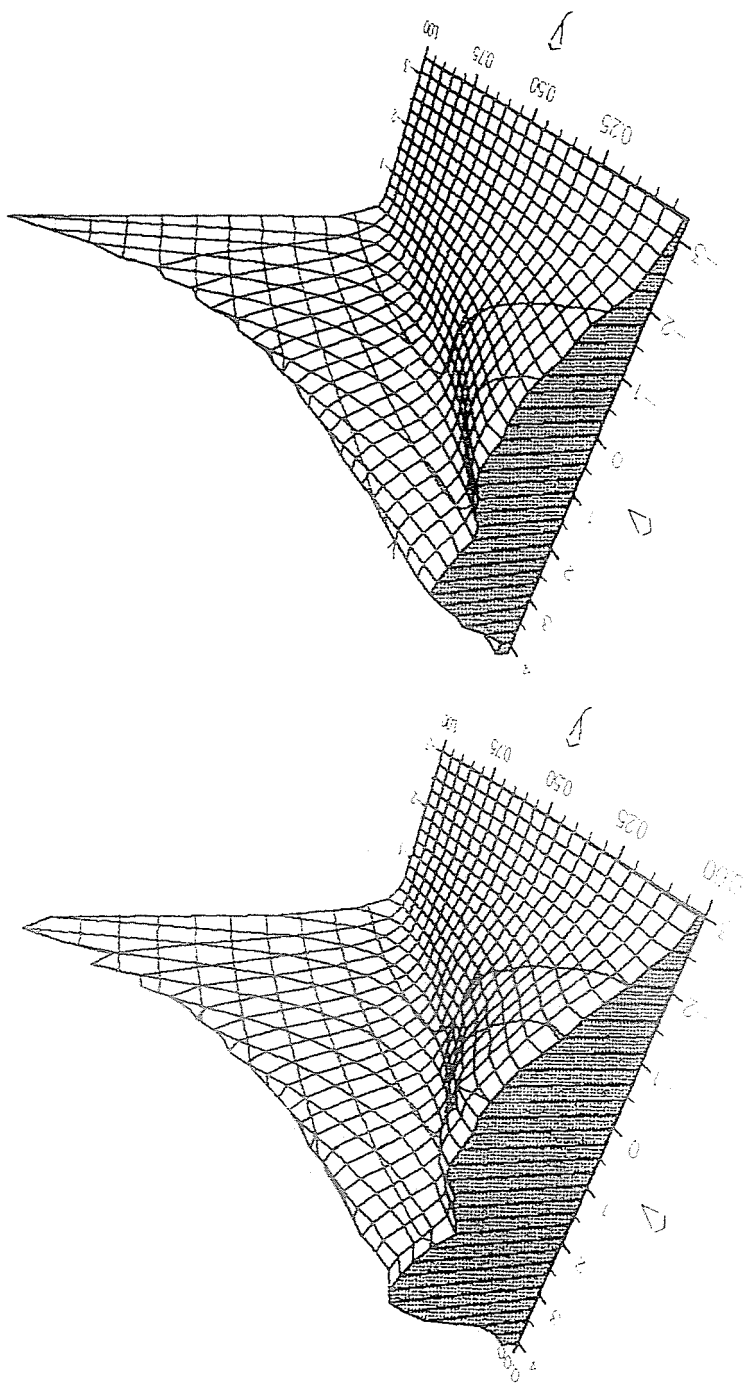


Fig. 10. Phase-space distribution for partially adsorbing boundary

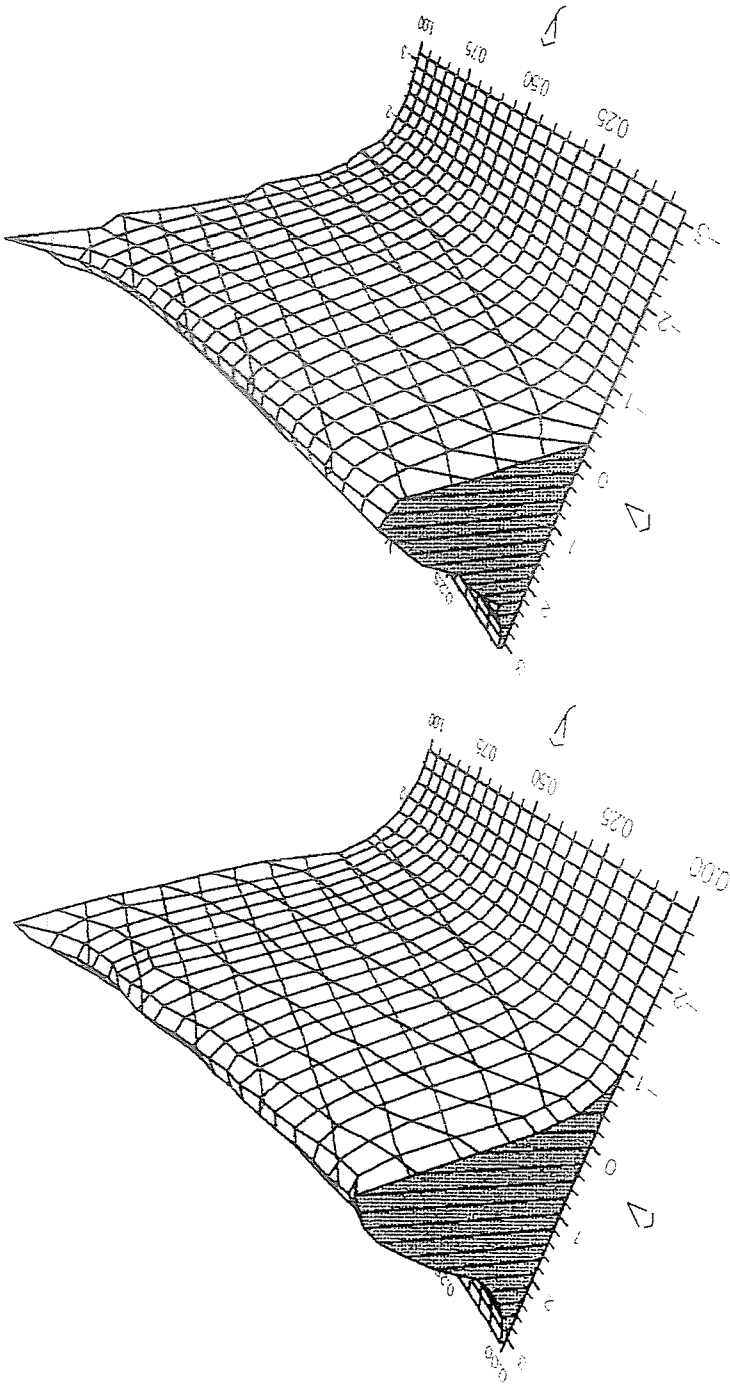


Fig. 11. Phase-space distribution for perfectly adsorbing boundary

References

- GARDINER, C. W., (1990): Handbook of Stochastic Methods, Springer-Verlag.
- GLADWELL, I. (1987): The NAG Library Boundary Value Codes; *Manchester University Numerical Analysis Report*, No. 135.
- KALLIO, G. A. - REEKS, M. W., (1989): A Numerical Simulation of Particle Deposition in Turbulent Boundary Layers, *Int. J. Multiphase Flow*, Vol. 15, No. 3, pp. 433-446.
- REEKS, M. W., (1991): On a Kinetic Equation for the Transport of Particles in Turbulent Flows, *Phys. Fluids A*, Vol. 3 No. 3, pp. 446-456.
- REEKS, M. W. - TANG, T. - HYLAND, K., - MCKEE, S. - SWAILES, D. C., (1991): ANALYTIC AND NUMERIC SOLUTIONS FOR A FOKKER-PLANCK TYPE TRANSPORT EQUATION, *Gas-Solid Flows ASME*, FED-VOL. 121, PP. 45-49.
- SWAILES, D. C. - REEKS, M. W. (1994a): Particle Deposition. Gravitational and surface effects, *Proc. 7th. workshop on Two-phase flow predictions*, Erlangen April 11-14, (to appear).
- SWAILES, D. C. - REEKS, M. W. (1994b): Particle Deposition from a Turbulent Flow. Part I: A Steady-state Model for High Inertia Particles *Phys. Fluids* Vol. 6, No. 10, pp. 3392-3403.